Complete Francis turbine flow simulation at Derbendikan power station

R. A. Saeed[1], V. Popov[2] & A. N. Galybin[2,3]
[1]*University of Sulaimani, Iraq*
[2]*Wessex Institute of Technology, UK*
[3]*Institute of Physics of the Earth, Russia*

Abstract

This paper presents the results of simulations of the complete three-dimensional fluid flow through the Spiral Casing, Stay Vane, Guide Vane, and then through the Francis turbine runner of the Derbendikan power station. To investigate the flow in the Francis turbine and also to identify the loads acting on the turbine blades, a three-dimensional model was prepared according to specifications provided. The results show that the maximum absolute pressure of 4.4×10^5 Pa is reached at the leading edge of the turbine runner and the maximum tangential velocity reaches 33 m/s in the turbine runner.
Keywords: Francis turbine runner, numerical simulation, CFD modelling.

1 Introduction

Generally the flow field in Francis turbines is quite complicated due to its three-dimensional nature and the curvature of the passages between runner blades. The complexity of the problem requires the application of numerical approaches which are capable of producing accurate results for flow velocity field and pressure distributions on the runner. The application of *CFD* is an efficient way for the analysis of fluid flow through hydraulic turbines [1]. Nava *et al.* [2] presented an application of *CFD* to compute the loads caused by water pressure on a blade of the Francis turbine runner. There is a satisfactory agreement between numerical simulations and experimental measurements as reported by Farhat *et al*. [4], who compared the flow simulation results and experimental data for the whole Francis turbine. Three-dimensional steady flow analysis of the flow passages from the entrance runner to the outlet in Francis turbine type has

WIT Transactions on Engineering Sciences, Vol 74, © 2012 WIT Press
www.witpress.com, ISSN 1743-3533 (on-line)
doi:10.2495/AFM120051

been reported by Ikeda *et al*. [5]. This analysis provides the distributed pressure and water velocity within the computational domain.

In this paper, the pressure distribution and flow velocity field were investigated by using Computational Fluid Dynamics (*CFD*) for specific operating condition. Detailed analysis of the fluid flow through the turbine runner is necessary in order to study the fluid flow conditions. For this purpose the Spiral Casing, Stay Vane, Guide Vane, Runner and upper part of the Draft tube have been considered. The corresponding model is shown in Figure 1.

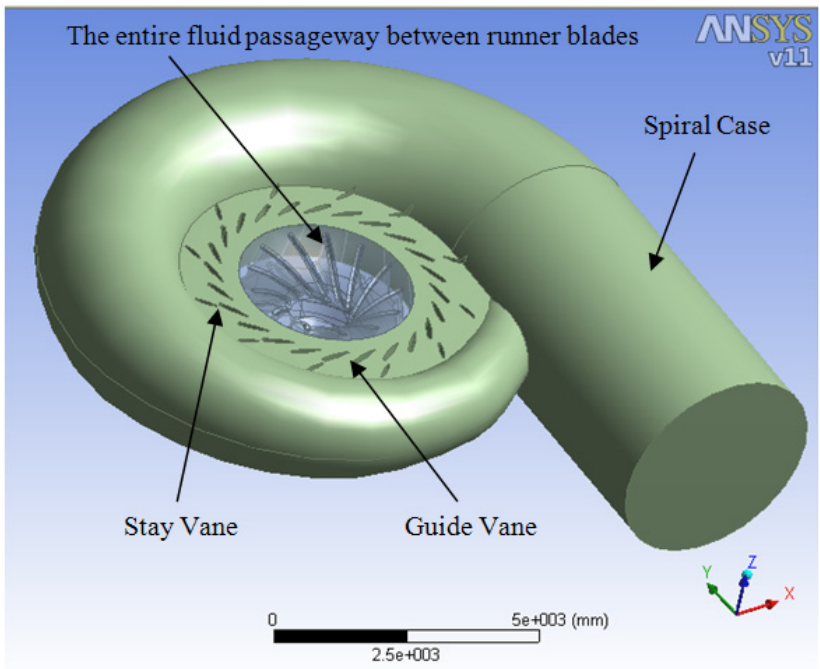

Figure 1: Geometrical model used in the simulation.

This work includes the analysis of the performance of the Francis turbine of Unit 2 in Derbendikan hydropower station; one of the major suppliers of electrical power generation in the north of Iraq- Kurdistan Region. The investigated turbine has the following data [7]: number of runner blades 13, number of guide vanes 24, rated head 80 *m*, power output at rated head 83 *MW*, discharge at rated head 113 m^3/s, rotational speed 187.5 *rpm*.

2 Flow simulations

The flow simulation of the Francis turbine runner is quite complicated and can be calculated only by using numerical methods. *CFD* simulation of the Francis turbine runner was performed to obtain pressure distribution and flow velocity

through the turbine runner. Following previous research [9, 10], for the computational domain, the Spiral Casing, Stay Vane, Guide Vane, Runner and upper part of the Draft tube is considered.

2.1 Geometrical model

The first step of flow simulation is building the geometrical model of the flow domain. According to the provided specifications from Derbendikan hydropower station a three-dimensional geometrical model has been created, as shown in Figures 1 and 2. The geometry of the fluid domain has been created on AutoCAD software and inserted into ANSYS software.

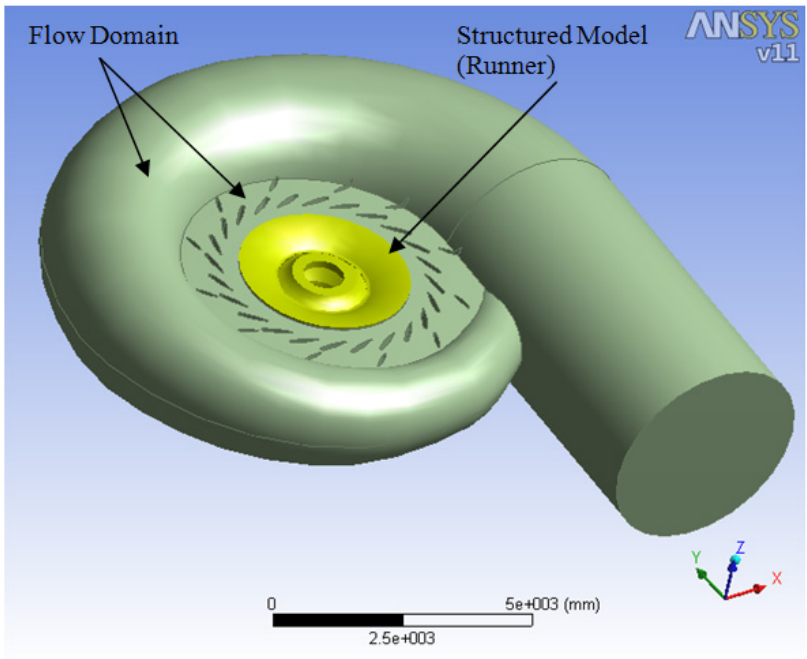

Figure 2: Flow domain and structured model.

As shown in the figure, the entire fluid passageway between the inlet from the Spiral Case side and the outlet from the draft tube side for the turbine is considered.

The flow in the runner was computed in the rotating frame of reference, while the flow in the stationary components was calculated in the stationary frame of reference. Figure 2 shows the detail of the connection between flow domains used for *CFD* simulations and Francis turbine runner model.

2.2 Discretization process

In this study, three-dimensional discretization has been used with the finite volume method (*FVM*) provided by the ANSYS CFX software. For the computational domain, unstructured 3D tetrahedral meshing has been employed, due to its flexibility when solving complex geometries, as shown in Figure 3. The whole computational mesh consists of 3,241,986 volumes and 628,677 nodes.

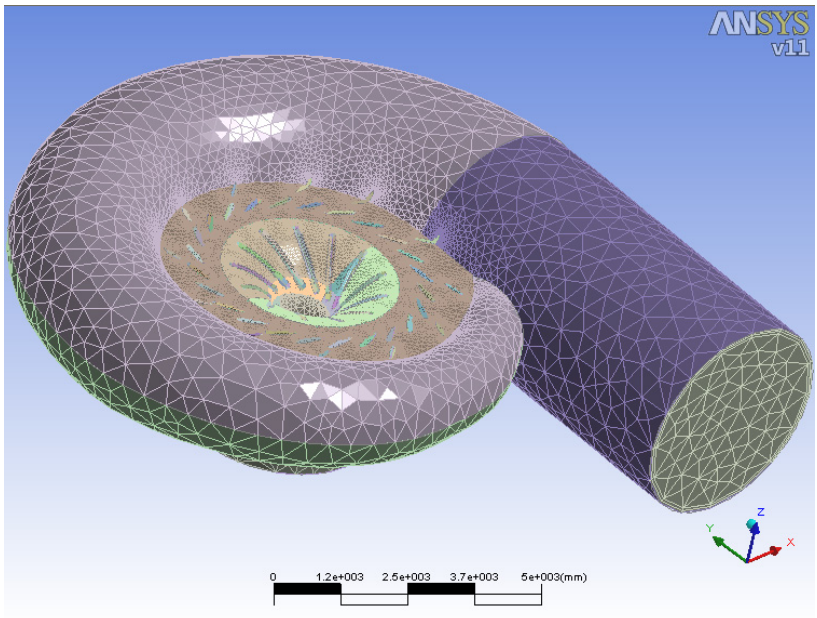

Figure 3: 3D structured grids of the computational domain.

2.3 Numerical modelling of turbulent fluid flow

The flow is considered to be viscous, incompressible and turbulent. The present paper focuses on 3-D Navier-Stokes simulations using the commercial code ANSYS CFX. The continuity equation and Reynolds-averaged Navier-Stokes (*RANS*) equation for incompressible flow have been used as governing equations in the following form [11]:

$$\frac{\partial U_i}{\partial X_i} = 0 \tag{1}$$

$$\frac{\partial U_i}{\partial t} + U_j \frac{\partial U_i}{\partial X_j} + \frac{1}{\rho}\frac{\partial P}{\partial X_i} - \frac{\partial}{\partial X_j}\left(\upsilon\left(\frac{\partial U_i}{\partial X_j} + \frac{\partial U_j}{\partial X_i}\right) - \tau_{ij}\right) = 0 \tag{2}$$

where U, p, υ and ρ are velocity, pressure, kinematic viscosity and density, respectively, and τ_{ij} are the components of the viscous stress tensor, also called the Reynolds Stress Tensor. The turbulent effects on the flow field are taken into account through the Reynolds Stresses τ_{ij} , those are calculated from the k-ε turbulence model, which is frequently used for modelling turbulent flow.

2.4 Boundary conditions

The computations assume steady state incompressible uniform fluid flow in normal direction in the entrance of Spiral Case. Total mass flow in stationary frame was specified at the inlet while static pressure was defined at the outlet boundary. Inlet boundary conditions at given performance point of the hydraulic turbine runner are derived from an operation condition which include discharge Q (82 m^3/s), where the Guide Vanes opening is 80%. Outlet boundary condition is defined to an opening with an average relative pressure to atmospheric pressure.

2.5 Resolution phase

In engineering applications in order to achieve convergence of the solution to an acceptable level, the residual is usually set between four to six orders of magnitude lower than the actual values [12]. Iterative methods are used to solve the corresponding system of algebraic equations, which allows one to characterize the accuracy of the approximation solution by analysing the residual. In this study, the *RMS* residuals settled to a steady state value within 100 iterations. The non-dimensional residual of the momentum and continuity equations was between 10^{-4} to 10^{-6}.

2.6 Results and discussion

Three-dimensional analyses of fluid flow through the Spiral Case, Stay and Guide Vanes and then through the turbine blades channel have been carried out. The distributions of pressure and water velocity within the computational domain are illustrated in the form of contour and streamlines that are generated with the ANSYS CFX postprocessor.

The variation of pressure distributions and tangential velocity in the computational domain obtained from the *CFD* analysis for specific operating conditions are plotted in a plane which is passing through the centre of Spiral Case and across the axis's of rotation as shown in Figure 3(A and B).

The symmetrical inflow to the runner in circumferential direction can be observed, which results in symmetrical distribution pressure from the uniform flow distribution of the runner inlet, as shown in Figure 4B. The tangential velocity increase has been detected at the lower ring, which is due to the smaller area at the distributor region, as evident in Figure 4A.

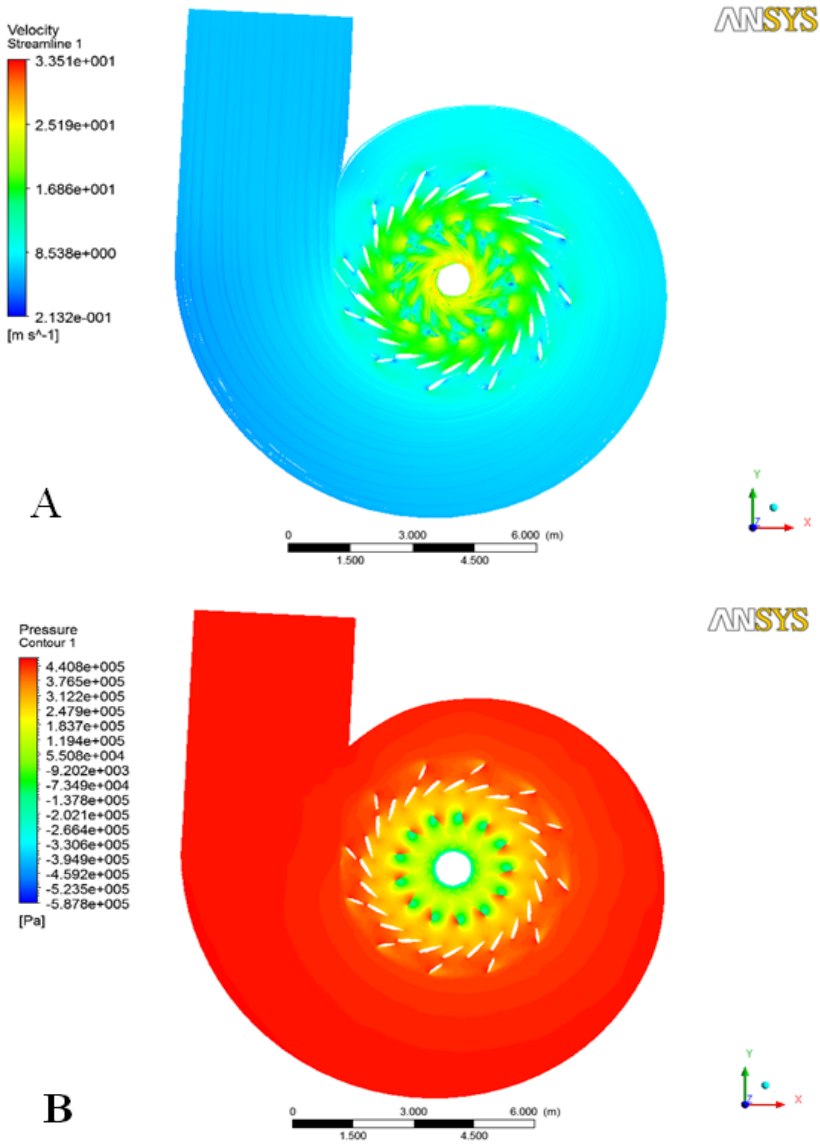

Figure 4: (A) Variation of tangential velocity [ms^{-1}] and (B) pressure distributions [Pa] in the computational domain.

Figure 5(A and B), show the streamlines of the tangential velocity and the runner surface pressure distributions in the plane passing through the centre of Spiral Case and parallel to the axis's of rotation. The tangential velocity component decreases on the blade at the leading edge, which is due to the sharp.bend of the flow in the stagnation regions near the blades, as observed in

Figure 5A. From Figure 5B, reduction from high pressure in the runner inlet to low pressure at the runner outlet is clearly observed. High magnitudes of water pressure are observed at the leading edge of the runner due to stagnation pressure on the blades, which results from the rapid decrease in the magnitude of the tangential velocity close to the bend of the flow.

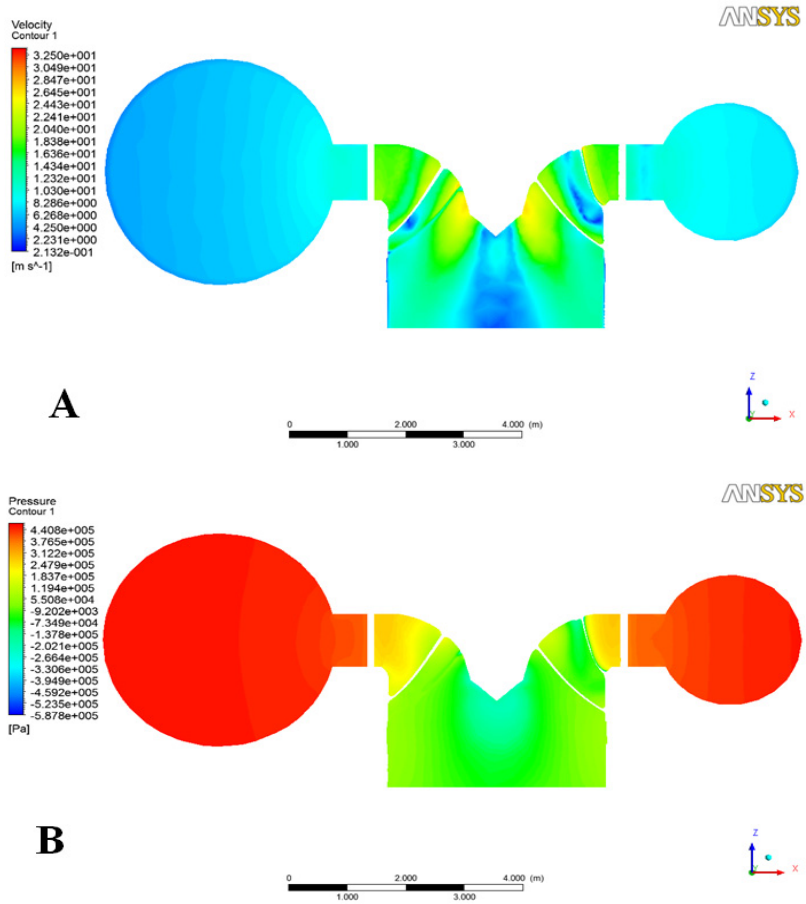

Figure 5: (A) Tangential velocity [ms^{-1}] and (B) the distribution of pressure [Pa] in the turbine.

At the top of the runner the pressure is quite high whereas at the bottom the pressure is low. The increasing pressure on the blades is clearly visible due to stagnation. The reduction of pressure on the runner blade suction side is explained by higher magnitudes of the velocity at the trailing edge. Also, the pressure differences from the pressure and suction side are high and these differences provide the torque on the shaft.

As illustrated in Figure 6, the flow is coming out from the spiral inlet to the upper part of the draft tube at the outlet. The flow is streamlined up to the runner outlet and recirculation is established in the draft tube. This is due to the change in the direction of the flow in the draft tube.

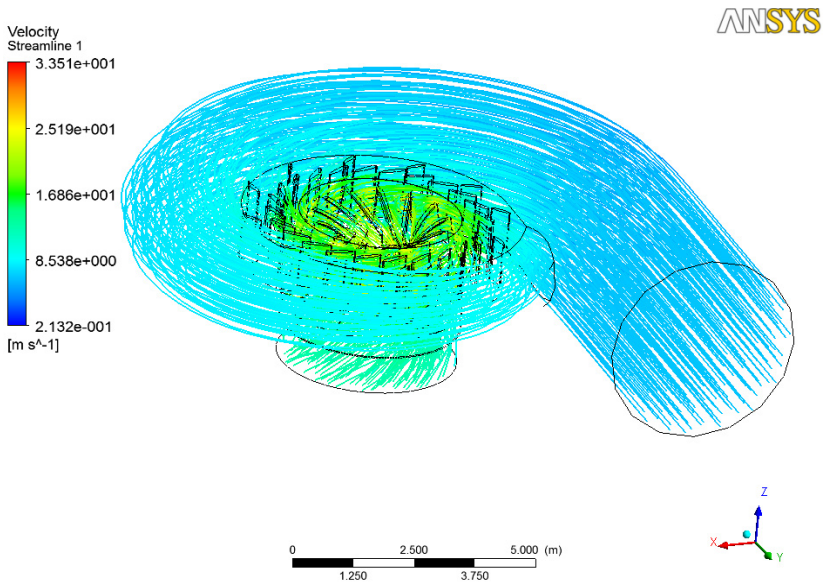

Figure 6: Tangential velocity [ms^{-1}] of the computational domain.

As observed in Figure 6, the flow direction is almost radial at the outlet region of the runner and it is nearly axial at the centre. While the recirculation region varies with the inlet boundary conditions, it increases gradually by decreasing velocity at the inlet. There is a sharp increase in the magnitude of velocity close to the trailing edge of the blade near the ring, due to the reduction of the area between the blade and the ring.

3 Conclusions

The simulation of the 3D steady-state fluid flow with moving reference frame in the entire Francis turbine from spiral case through stay vanes, wicket gates, and runner down to the draft tube is presented. The flow field simulation needs to include the entire flow passage to accurately model the runner surface pressure distributions and the streamlines of tangential velocity. Both these characteristics have been examined for a specific operation condition. Numerical simulation of the entire Francis turbine flow shows clearly the influence of the operation condition on the variation of pressure distributions and tangential velocity in the computational domain. The results show good agreement with the previous studies. The pressure profiles are used further to study stresses in the runner.

References

[1] Avellan, F., Etter, S., Gummer, J. H., Seidel, U., 2000, "Dynamic Pressure Measurements on a Model Turbine Runner and Their Use in Preventing Runner Fatigue Failure", 20th IAHR Symposium, Charlotte, North Carolina, USA.

[2] Nava, J. M. F., Gómez, O. D., Hernández J. A. R. L., Flow induced stresses in a Francis runner using ANSYS, International ANSYS Conference Proceedings, 2006.

[3] Bjorndal, H., Moltubakk, T., Aunemo, H., 2001, "Flow Induced Stresses in a Medium Head Francis Runner - Strain gauge measurements in an operating plant and comparison with Finite Element Analysis", 10th International Meeting of the IAHR Work Group on the Behaviour of Hydraulic Machinery under Steady Oscillatory Conditions, Trondheim, Norway.

[4] Farhat, M., S. Natal, Avellan, F., Paquet, F., Lowys, Py., Couston, M., 2002, "Onboard Measurements of Pressure and Strain Fluctuations in a Model of Low Head Francis Turbine Part 2 : Measurements and Preliminary Analysis Results", Proceedings of the 21st IAHR Symposium on Hydraulic Machinery and Systems, Lausanne, pp. 873-880.

[5] Ikeda, K., Inagaki, M., Niikura, K., Oshima, K., 700-m 400-MW Class Ultrahigh-head Pump Turbine, Hitachi Review Vol. 49, No. 2, pp. 81-87, 2000

[6] Farhat, M., Avellan, F., Seidel, U., 2002, "Pressure Fluctuation Measurements in Hydro Turbine Models", 9th International Symposium on Transport Phenomena and Dynamics of Rotating Machinery, Honolulu, Hawaii, USA.

[7] Fattah, S. S., Khoshnaw, F. M., Saeed, R. A., 2005, "An Investigation about Preventing Cavitation Damage and Fatigue Failure in Derbendikhan Power Station", Fluid Structure Interaction and Moving Boundary Problems, Spain, Vol. 84, pp. 97-106.

[8] Friziger, J. H., 2002. Computational Methods for Fluid Dynamics. Springer, New York, USA.

[9] Čarija Z., Mrša, Z., 2003, "Complete Francis Turbine Flow Simulation for the Whole Range of Discharges", 4th International Congress, of Croatian Society of Mechanics, Bizovac, Croatia, pp. 105-111.

[10] Ruofu, X., Zhengwei, W., Yongyao, L., 2008, "Dynamic Stresses in a Francis Turbine Runner Based on Fluid-Structure Interaction Analysis", Tsinghua Science and Technology, Vol. 13, No. 5, pp. 587-592.

[11] Ruprecht, A., Heitele, M., Helmrich, T., Moser, W., Aschenbrenner, T., 2000, "Numerical simulation of a complete Francis turbine including unsteady rotor/stator interactions", Proceedings of the 20th IAHR.

[12] Hirsch, C., 2007, Numerical Computation of Internal and External Flows, John Wiley and Sons, Ltd, Oxford, Great Britain.